

1 **A Ferromagnetic Salicylaldoximate/Azide Mn<sup>II</sup><sub>2</sub>Mn<sup>III</sup><sub>6</sub> Cluster with an S = 17 Ground State and a**  
2 **Single-Molecule-Magnet Response**

3  
4  
5  
6  
7 R. Vicente,<sup>\*,†</sup> M. S. El Fallah,<sup>†</sup> B. Casanovas,<sup>†</sup> M. Font-Bardia,<sup>‡</sup> and A. Escuer<sup>\*,†</sup>  
8  
9  
10

11 <sup>†</sup>Department de Química Inorgànica i Orgànica, Secció Inorgànica and Institut de Nanociència i  
12 Nanotecnologia, Universitat de Barcelona, Martí Franquès 1–11, 08028 Barcelona, Spain

13 <sup>‡</sup>Departament de Mineralogia, Cristal·lografia i Dipòsits Minerals and Unitat de Difracció de R-X,  
14 Centre Científic i Tecnològic de la Universitat de Barcelona, Universitat de Barcelona, Solé i Sabarís 1-  
15 3, 08028 Barcelona, Spain

16  
17  
18  
19 Ramón Vicente: [rvicente@ub.edu](mailto:rvicente@ub.edu)

20 Albert Escuer: [albert.escuer@ub.edu](mailto:albert.escuer@ub.edu)  
21  
22  
23

24 **ABSTRACT:**

25 One new Mn<sup>II</sup><sub>2</sub>Mn<sup>III</sup><sub>6</sub> cluster exhibiting an S = 17 spin ground state and single-molecule-magnet  
26 properties has been designed linking Mn<sup>III</sup><sub>3</sub>-salicylaldoximate triangles and tetracoordinated Mn<sup>II</sup> cations  
27 by means of end-on azido bridges. The ferromagnetic coupling has been rationalized as a function of  
28 their structural parameters.  
29

30 After the discovery of the first members of the  $\text{Mn}^{\text{III}}_6$  family of single molecule magnets (SMMs)  
31 employing the salicylaldoxime ( $\text{H}_2\text{salox}$ ) ligand<sup>1</sup> and further systematic study in the last 10 years by  
32 Brechin et al.,<sup>2-11</sup>  $\{\text{Mn}^{\text{III}}_3(\mu_3\text{-O})\}$  triangular fragments with salicyloximato side bridges have been one of  
33 the most fruitful and better studied systems in the search for a SMM response. The factors that control  
34 the sign and magnitude of the magnetic interaction inside the triangular units were rationalized as a  
35 function of the  $\text{Mn}^{\text{III}}\text{-N-O-Mn}^{\text{III}}$  torsion angle, establishing the border between ferromagnetic (FM) and  
36 antiferromagnetic (AF) interaction around  $31^\circ$ .<sup>4,5</sup>

37 The ground state for a  $\{\text{Mn}^{\text{III}}_3(\mu_3\text{-O})\}$  triangle is restricted to the  $S = 0-6$  range, but the hexanuclear  
38 systems, consisting of two linked triangles by means of  $\eta^2:\eta^1:\eta^1:\mu_3$ -oximato bridges, can reach the larger  
39  $S = 12$  ground state (Chart 1). It is worth noting that for these systems the easy axes of the  $\text{Mn}^{\text{III}}$  cations  
40 are roughly parallel, and they reached the largest energy barrier to magnetization reversal for d  
41 transition-metal clusters.<sup>6</sup> In addition to the  $\text{Mn}^{\text{III}}_3$  and  $\text{Mn}^{\text{III}}_6$  cores, other molecular clusters, based in the  
42  $\{\text{Mn}^{\text{III}}_3(\mu_3\text{-O})\}$  fragment, are those consisting of four stacked triangles<sup>12</sup> ( $\text{Mn}^{\text{III}}_{12}$ ),  $\text{Mn}^{\text{II}}$  bicapped  
43 triangles<sup>13,14</sup> with a  $\text{Mn}^{\text{II}}_2\{\text{Mn}^{\text{III}}_3(\mu_3\text{-O})\}$  core, or  $\text{Mn}^{\text{II}}$  bicapped hexanuclears with a  $\text{Mn}^{\text{II}}_2\{\text{Mn}^{\text{III}}_6(\mu_3\text{-O})_2\}$ <sup>15-17</sup>  
44 core. The presence of two additional  $\text{Mn}^{\text{II}}$  cations can reduce or increase the  $S$  ground state by  
45 up to five units as a function of the sign and magnitude of the magnetic interactions. In fact,  
46 Hendrickson proved experimentally that the pentanuclear  $\text{Mn}^{\text{II}}_2\{\text{Mn}^{\text{III}}_3(\mu_3\text{-O})\}$  core can reach up to the  
47 maximum  $S = 11$  ground state,<sup>14</sup> whereas only AF interactions between the  $\text{Mn}^{\text{II}}$  and  $\text{Mn}^{\text{III}}$  cations have  
48 been found until now for the  $\text{Mn}^{\text{II}}_2\{\text{Mn}^{\text{III}}_6(\mu_3\text{-O})_2\}$  core, resulting in  $S = 1$  and  $7$  ground states.<sup>15-17</sup>  
49 On the basis of these premises, we have designed the synthesis of one new octanuclear compound with a  
50  $\text{Mn}^{\text{II}}_2\{\text{Mn}^{\text{III}}_6(\mu_3\text{-O})_2\}$  core with the goal of obtaining FM interactions between the inner hexanuclear  
51 fragment and the capping  $\text{Mn}^{\text{II}}$  cations and reaching the  $S = 17$  record ground state for this wide family  
52 of complexes. The reaction of  $\text{H}_2\text{salox}$ , sodium azide, and manganese chloride in a methanolic medium,  
53 employing  $\text{Pr}_4\text{NOH}$  as a base, yields compound  $(\text{Pr}_4\text{N})_2[\text{Mn}_2^{\text{II}}\text{Mn}_6^{\text{III}}(\text{O})_2(\text{salox})_6(\text{N}_3)_6(\text{Cl})_2(\text{H}_2\text{O})_2] \cdot 2\text{H}_2\text{O}$   
54 ( $1 \cdot 2\text{H}_2\text{O}$ ; Supporting Information, synthetic details). Analysis of its magnetic properties reveals a SMM  
55 response with a medium energy barrier. Complex 1 can be described as two stacked  $\{\text{Mn}^{\text{III}}_3(\mu_3\text{-O})(\text{salox})_3\}$   
56 triangles bicapped by  $\text{Mn}^{\text{II}}$  cations (Figure 1, and BSV calculations in Table S1). The  $\text{Mn}^{\text{III}}$   
57 cations are linked by  $\text{salox}^{2-}$  ligands, four of them in the main plane of the triangular subunits in its  
58  $\eta^1:\eta^1:\eta^1:\mu^2$  coordination mode and two in its  $\eta^1:\eta^2:\eta^1:\mu^3$  mode, connecting both triangles.  $\text{Mn}1$  and  $\text{Mn}3$   
59 are hexacoordinated, whereas  $\text{Mn}2$  shows a square-pyramidal environment, with weak contact with the  
60 phenoxo  $\text{O}3'$  atom. Each triangular subunit is capped by one  $\text{Mn}^{\text{II}}$  cation, linked by means of three end-  
61 on azido bridges with similar  $\text{Mn}^{\text{II}}\text{-N}_{\text{azido}}\text{-Mn}^{\text{III}}$  bond angles close to  $104.0^\circ$ . The  $\text{Mn}^{\text{II}}$  cation is  
62 tetraordinated, and the coordination sphere is fulfilled with one  $\text{Cl}^-$  anion.  $\text{Mn-N-O-Mn}$  torsion  
63 angles are relatively low with  $13.7(5)^\circ$ ,  $25.5(5)^\circ$ , and  $32.1(4)^\circ$  values. Charge balance is achieved with  
64 two  $\text{Pr}_4\text{N}^+$  cations, which efficiently isolate the octanuclear clusters. The only intermolecular interaction  
65 involves the coordinated and crystallization water molecules and one azidoNatom. Additional plots and  
66 structural data can be found in Tables S2 and S3 and Figures S1 and S2.

67 The room temperature  $\chi_{\text{M}}T$  value is  $28.96 \text{ cm}^3 \cdot \text{mol}^{-1} \cdot \text{K}$ , slightly larger than the expected value for two  
68  $\text{Mn}^{\text{II}}$  and six  $\text{Mn}^{\text{III}}$  noninteracting ions ( $g = 2.00$ ; Figure 2). Upon cooling,  $\chi_{\text{M}}T$  increases up to a  
69 maximum value of  $100.6 \text{ cm}^3 \cdot \text{mol}^{-1} \cdot \text{K}$  at  $5 \text{ K}$ , and below this temperature,  $\chi_{\text{M}}T$  decays to a final value of  
70  $85.4 \text{ cm}^3 \cdot \text{mol}^{-1} \cdot \text{K}$  at  $2 \text{ K}$ . The most simplified coupling scheme to describe the system requires four  $J$   
71 constants, assuming  $J_1$  as the intertriangle interaction,  $J_2$  and  $J_3$  as the interactions mediated by the  $\text{Mn-O-N-Mn}$   
72 pathways with torsions larger or lower than  $30^\circ$ , respectively, and  $J_4$  as the  $\text{Mn}^{\text{II}} \cdots \text{Mn}^{\text{III}}$   
73 interaction mediated by end-on azido bridges (Figure S3).

74 The system was fitted<sup>18</sup> isotropically in the  $25-300 \text{ K}$  range of temperature to avoid low-temperature  
75 effects as zero-field splitting. Best-fit parameters under these conditions were  $J_1 = +3.9 \text{ cm}^{-1}$ ,  $J_2 =$   
76  $14.0 \text{ cm}^{-1}$ ,  $J_3 = -2.7 \text{ cm}^{-1}$ ,  $J_4 = +7.4 \text{ cm}^{-1}$ , and  $g = 1.88$  with  $R = 6.0 \times 10^{-4}$ , suggesting an  $S = 17$   
77 ground state. As will be further discussed, the sign and magnitude of the  $J$  and  $g$  constants lie in the  
78 normal range for these kinds of systems, but absolute values of  $J$  are obviously poorly reliable as a  
79 consequence of the simplified fit procedure.

80 Magnetization measurements at 2 K in the 0–5 T field range show a maximum unsaturated value  
81 equivalent to 28.2 electrons, which can be fitted<sup>18</sup> to the maximum spin  $S = 17$  for  $g = 1.87$  and  $D \approx$   
82  $0.15 \text{ cm}^{-1}$  (Figure 2). In light of these results and the more reliable further fit of the reduced  
83 magnetization, which gives a  $D$  value of  $-0.12 \text{ cm}^{-1}$  (Figure S4), alternating-current measurements were  
84 performed in the 1488–10 Hz range of frequencies.

85 Well-defined  $\chi''$  peaks in the 3.96–2.85 K range were observed (Figure 3). The Arrhenius fit of the peak  
86 maxima gives  $E_a = 35.2 \text{ cm}^{-1}$ ,  $\tau_0 = 3.25 \times 10^{-10} \text{ s}$ , and  $D = -0.12 \text{ cm}^{-1}$ , in excellent agreement with the  $D$   
87 value obtained from the reduced magnetization measurement and indicating that tunnelling relaxation is  
88 not operative. Measurements at 2 K do not show magnetic hysteresis.

89 Nevertheless, an interesting question arises from analysis of the structural data: following the rule of the  
90  $\text{Mn}^{\text{II}}\text{-N-O-Mn}^{\text{III}}$  torsion angle<sup>5</sup> and compared with  $\text{Mn}^{\text{III}}_6$  complexes with a similar range of torsion  
91 angles (summarized in Table S4),<sup>10,19–21</sup> the inner hexanuclear unit should have an  $S = 4$  local spin and,  
92 *apparently*, complex 1 should only reach  $S = 9$  if the interaction with the  $\text{Mn}^{\text{II}}$  cations was FM. Thus,  
93 *why does this complex reach its maximum spin?*

94 The answer requires detailed analysis of selected bond parameters of the related octanuclear  
95  $[\text{Mn}_2^{\text{II}}\text{Mn}_6^{\text{III}}(\text{O})_2(\text{naphtsalox})_6(\text{N}_3)_6(\text{MeOH})_8]$  and  $[\text{Mn}_2^{\text{II}}\text{Mn}_6^{\text{III}}(\text{O})_2(\text{Mesao})_6(\text{N}_3)_6(\text{MeOH})_8]$  clusters  
96 (CCDC codes CIGYIB and CIGYOH)<sup>15,16</sup> and the pentanuclear  $[\text{Mn}_2^{\text{II}}\text{Mn}_3^{\text{III}}(\text{O})\text{-(salox)}_3(\text{N}_3)_6\text{X}_2]^{2-}$  ( $X =$   
97 Cl, Br) and  $[\text{Mn}_2^{\text{II}}\text{Mn}_3^{\text{III}}(\text{O})(\text{Mesao})_3(\text{N}_3)_6\text{Cl}_2]^{2-}$  complexes,<sup>13,14</sup> (CCDC codes TEZNES, WAJKOJ, and  
98 WAJKUP; Table S5). If the capping  $\text{Mn}^{\text{II}}$  cation is octahedrally coordinated, as occurs for CIGYIB and  
99 CIGYOH, the  $\text{Mn}^{\text{II}}\text{-N}_{\text{azido}}$  bond distances are larger than  $2.2 \text{ \AA}$ , the  $\text{N}_{\text{azido}}\text{-Mn}^{\text{II}}\text{-N}_{\text{azido}}$  angles are close to  
100  $90^\circ$ , and the  $\text{Mn}^{\text{II}}\text{-N}_{\text{azido}}\text{-Mn}^{\text{III}}$  bond angles are close to  $120^\circ$ . When the capping  $\text{Mn}^{\text{II}}$  cation is  
101 tetrahedrally coordinated, the  $\text{N}_{\text{azido}}\text{-Mn}^{\text{II}}\text{-N}_{\text{azido}}$  bond angles increase up to  $110^\circ$  and the remainder of  
102 the bond parameters are also modified:  $\text{Mn}^{\text{II}}\text{-N}_{\text{azido}}$  distances become  $0.1 \text{ \AA}$  shorter, axial  $\text{Mn}^{\text{III}}\text{-N}_{\text{azido}}$   
103 distances increase, the  $\text{Mn}^{\text{II}}\text{-N}_{\text{azido}}\text{-Mn}^{\text{III}}$  bond angles decrease below  $110^\circ$ , and the  $\text{Mn}^{\text{II}}$  cation is closer  
104 to the centroid of the  $\text{Mn}^{\text{III}}_3$  plane, giving a compressed  $\{\text{Mn}^{\text{II}}(\text{N}_3)_3\text{Mn}^{\text{III}}_3\}$  fragment (Figure 4).

105 End-on azido bridges usually induce FM interaction,<sup>22</sup> but for large  $\text{Mn-N-Mn}$  bond angles, it becomes  
106 AF, as was demonstrated by Alvarez et al.<sup>23</sup> Tetrahedral coordination of the capping  $\text{Mn}^{\text{II}}$  for 1 leads to  
107  $\text{Mn}^{\text{II}}\text{-N}_{\text{azido}}\text{-Mn}^{\text{III}}$  bond angles in the typical range of FM interactions.

108 When the oximate torsion and azide bond angle rules are combined, the  $S$  ground state for the systems  
109 in which the interactions inside the  $\{(\mu_3\text{-O})\text{Mn}^{\text{III}}_3\}$  units are FM is trivial:  $S$  ground states become a  
110 combination of the local  $S_L$  spin of the inner hexanuclear or trinuclear fragments and the  $5/2$  spins of  
111 each  $\text{Mn}^{\text{II}}$ , and thus applying  $S = |S_L \pm 5/2 \pm 5/2|$ , we obtain  $|12 - 5/2 - 5/2| = 7$  for CIGYOH,  $|6 + 5/2$   
112  $+ 5/2| = 11$  for TEZNES or WAJKOJ, and  $|6 - 5/2 + 5/2| = 6$  for WAJKUP, in full agreement with the  
113 experimental values (Table S5). In contrast, for the octanuclear systems with  $S = 4$  local spin for the  
114 inner hexanuclear unit, the overall  $S$  ground state is a function of the dominant interaction, and in that  
115 case, the  $S = |S_L \pm 5/2 \pm 5/2|$  sum is no longer applicable because all intermediate  $S$  ground states are  
116 possible. In fact, if the  $\text{Mn}^{\text{II}}\text{-Mn}^{\text{III}}$  interaction is AF and dominant, the ground state will be  $S = 7$ , and if  
117 this interaction is FM and dominant, the ground state will be  $S = 17$ . In contrast, if the  $\text{Mn}^{\text{II}}\text{-Mn}^{\text{III}}$   
118 interaction is weakly AF, the ground state must be  $S = 1$ , as occurs for the octanuclear complex CIGYIB  
119 (Figure S5).

120 In conclusion, we have reported a new member of the  $\text{Mn}^{\text{II}}_2\text{Mn}^{\text{III}}_6$  family of clusters based on bicapped  
121 stacked  $\text{Mn}^{\text{III}}$  triangles. The new system is FM, reaching the limit of the  $S = 17$  ground state, and it is  
122 moderately anisotropic and exhibits a SMM response with  $E_a = 35 \text{ cm}^{-1}$ . The FM response is attributed  
123 to a subtle combination of factors such as the tetrahedral environment of the  $\text{Mn}^{\text{II}}$  cation and the end-on  
124 azido bridges with low  $\text{Mn}^{\text{II}}\text{-N-Mn}^{\text{III}}$  bond angles.

125

126 **References**

- 127
- 128 Miliou, C. J.; Raptopoulou, C. P.; Terzis, A.; Lloret, F.; Vicente, R.; Perlepes, S. P.; Escuer, A. *Angew. Chem., Int. Ed.* 2004,
- 129 43, 210–212.
- 130 Miliou, C. J.; Vinslava, A.; Wood, P. A.; Parsons, S.; Wernsdorfer, W.; Christou, G.; Perlepes, S. P.; Brechin, E. K. *J. Am.*
- 131 *Chem. Soc.* 2007, 129, 8–9.
- 132 Miliou, C. J.; Vinslava, A.; Wernsdorfer, W.; Prescimone, A.; Wood, P. A.; Parsons, S.; Perlepes, S. P.; Christou, G.; Brechin,
- 133 E. K. *J. Am. Chem. Soc.* 2007, 129, 6547–6561.
- 134 Miliou, C. J.; Inglis, R.; Vinslava, A.; Bagai, R.; Wernsdorfer, W.; Parsons, S.; Perlepes, S. P.; Christou, G.; Brechin, E. K. *J.*
- 135 *Am. Chem. Soc.* 2007, 129, 12505–12511.
- 136 Miliou, C. J.; Inglis, R.; Bagai, R.; Wernsdorfer, W.; Collins, A.; Moggach, S.; Parsons, S.; Perlepes, S. P.; Christou, G.;
- 137 Brechin, E. K. *Chem. Commun.* 2007, 3476–3478.
- 138 Miliou, C. J.; Vinslava, A.; Wernsdorfer, W.; Moggach, S.; Parsons, S.; Perlepes, S. P.; Christou, G.; Brechin, E. K. *J. Am.*
- 139 *Chem. Soc.* 2007, 129, 2754–2755.
- 140 Miliou, C. J.; Piligkos, S.; Brechin, E. K. *Dalton Trans.* 2008, 1809–1817.
- 141 Inglis, R.; Miliou, C. J.; Jones, L. F.; Piligkos, S.; Brechin, E. K. *Chem. Commun.* 2012, 48, 181–190.
- 142 Martinez-Lillo, J.; Tomsa, A. R.; Li, Y.; Chamoreau, L. M.; Cremades, E.; Ruiz, E.; Barra, A. L.; Proust, A.; Verdaguier, M.;
- 143 Gouzerh, P. *Dalton Trans.* 2012, 41, 13668–13681.
- 144 Martinez-Lillo, J.; Dolan, N.; Brechin, E. K. *Dalton Trans.* 2013, 42, 12824–12827.
- 145 Martinez-Lillo, J.; Dolan, N.; Brechin, E. K. *Dalton Trans.* 2014, 43, 4408–4414.
- 146 Cordero, B.; Roubeau, O.; Teat, S. J.; Escuer, A. *Dalton Trans.* 2011, 40, 7127–7129.
- 147 Yang, C.-I.; Wernsdorfer, W.; Lee, G.-H.; Tsai, H.-L. *J. Am. Chem. Soc.* 2007, 129, 456–457.
- 148 Feng, P. L.; Stephenson, C. J.; Amjad, A.; Ogawa, G.; del Barco, E.; Hendrickson, D. N. *Inorg. Chem.* 2010, 49, 1304–1306.
- 149 Miliou, C. J.; Inglis, R.; Vinslava, A.; Prescimone, A.; Parsons, S.; Perlepes, S. P.; Christou, G.; Brechin, E. K. *Chem.*
- 150 *Commun.* 2007, 2738–2740.
- 151 Miliou, C. J.; Inglis, R.; Jones, L. F.; Prescimone, A.; Parsons, S.; Wernsdorfer, W.; Brechin, E. K. *Dalton Trans.* 2009,
- 152 2812–2822.
- 153 Escuer, A.; Cordero, B.; Font-Bardia, M.; Teat, S. J.; Roubeau, O. *Eur. J. Inorg. Chem.* 2016, 2016, 1232–1241.
- 154 PHI program: Chilton, N. F.; Anderson, R. P.; Turner, L. D.; Soncini, A.; Murray, K. S. *J. Comput. Chem.* 2013, 34,
- 155 1164–1175.
- 156 Inglis, R.; Jones, L. F.; Miliou, C. J.; Datta, S.; Collins, A.; Parsons, S.; Wernsdorfer, W.; Hill, S.; Perlepes, S. P.; Piligkos, S.;
- 157 Brechin, E. K. *Dalton Trans.* 2009, 3403–3412.
- 158 Holynska, M.; Dehnen, S. Z. *Anorg. Allg. Chem.* 2012, 638, 763–769.
- 159 Inglis, R.; Dalgarno, S. J.; Brechin, E. K. *Dalton Trans.* 2010, 39, 4826–4831.
- 160 Escuer, A.; Esteban, J.; Perlepes, S. P.; Stamatatos, T. C. *Coord. Chem. Rev.* 2014, 275, 87–129.
- 161 Ruiz, E.; Cano, J.; Alvarez, S.; Alemany, P. J. *Am. Chem. Soc.* 1998, 120, 11122–11129.
- 162

163 **Legends to figures**

164

165 Chart 1. Isolated, Stacked, or Capped  $\text{Mn}^{\text{III}}$ -Salox Triangles and Their Range of S Ground States<sup>a</sup>

166 <sup>a</sup>Color key:  $\text{Mn}^{\text{II}}$ , orange;  $\text{Mn}^{\text{III}}$ , dark green; O, red; N, navy blue.

167

168 Figure 1. Labelled plot of the core of compound 1.

169

170 Figure 2.  $\chi_{\text{M}}T$  product for compound 1. Inset: magnetization plot at 2 K. Solid lines show the best  
171 obtained fits.

172

173 Figure 3. Alternating-current measurements for compound 1. Inset: Arrhenius plot from the position of  
174 the  $\chi''$  peaks.

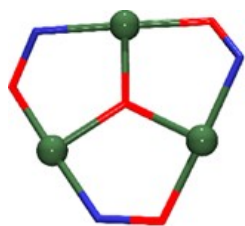
175

176 Figure 4. Triangular  $\{\text{Mn}^{\text{III}}_3(\mu_3\text{-O})(\text{oximate})_3\}$  fragments with end-on azido bridges linking an additional  
177  $\text{Mn}^{\text{II}}$  cation in octahedral or tetrahedral environments.

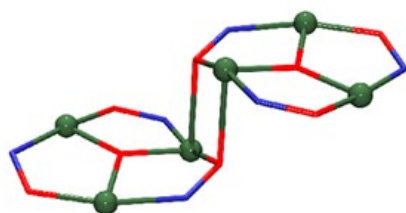
178

179  
180  
181

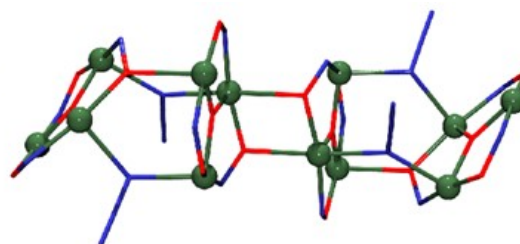
CHART 1



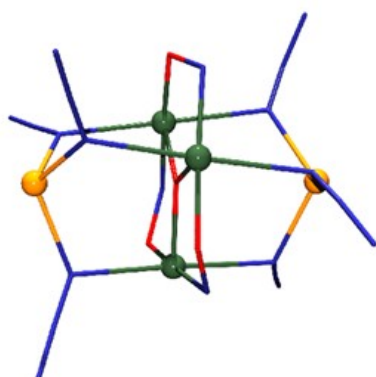
$S = 0 - 6$



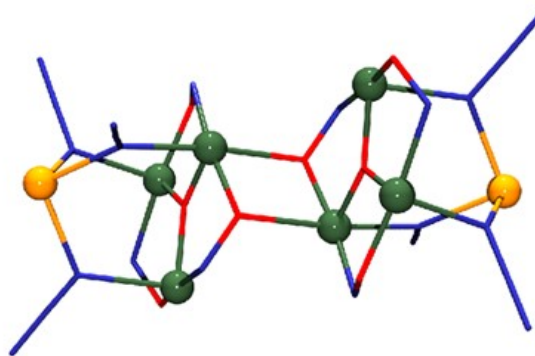
$S = 4 - 12$



$S = 8$



$S = 6, 11$



$S = 1, 7$

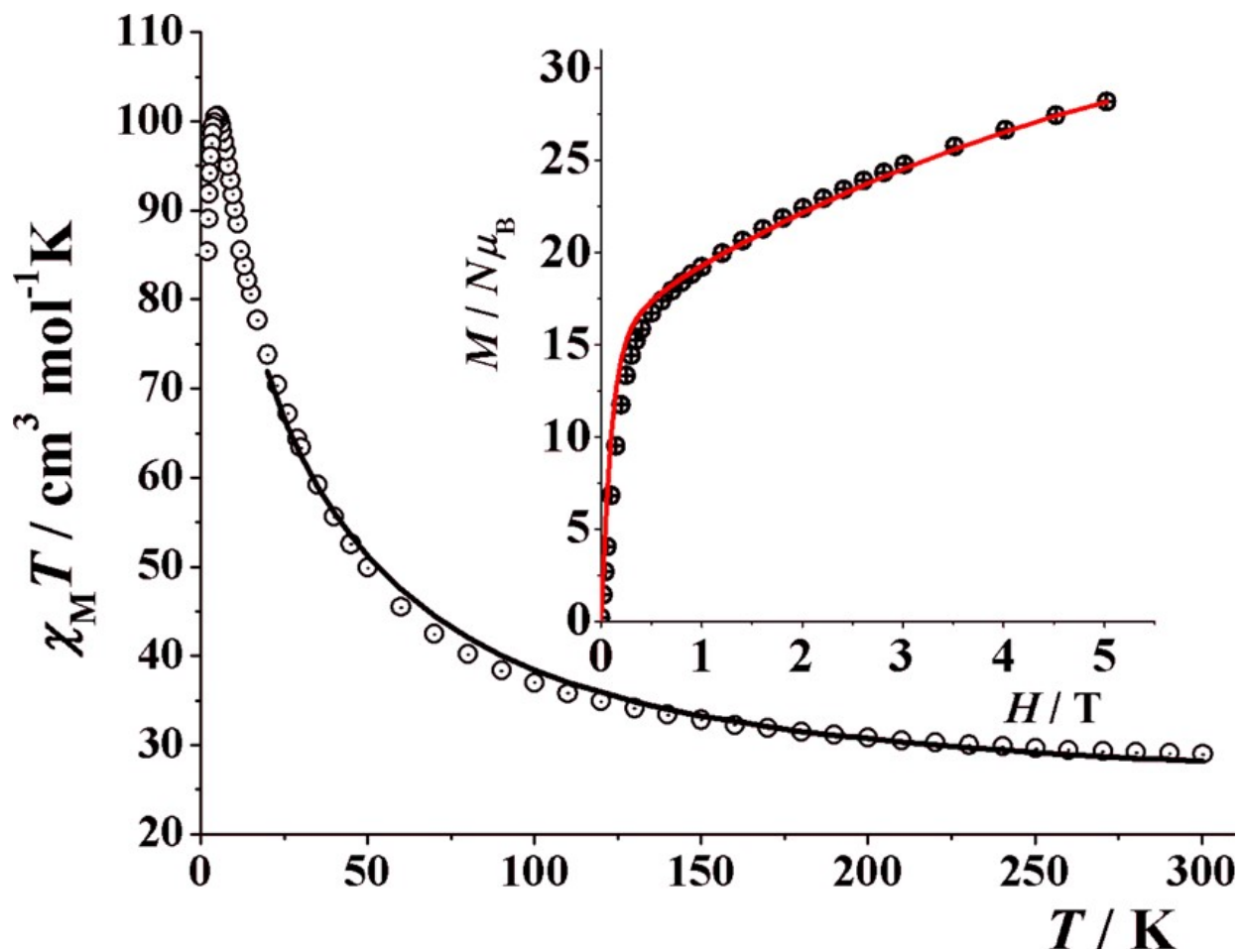
182  
183

184  
185  
186  
187  
188

**FIGURE 1**

189  
190  
191  
192

FIGURE 2

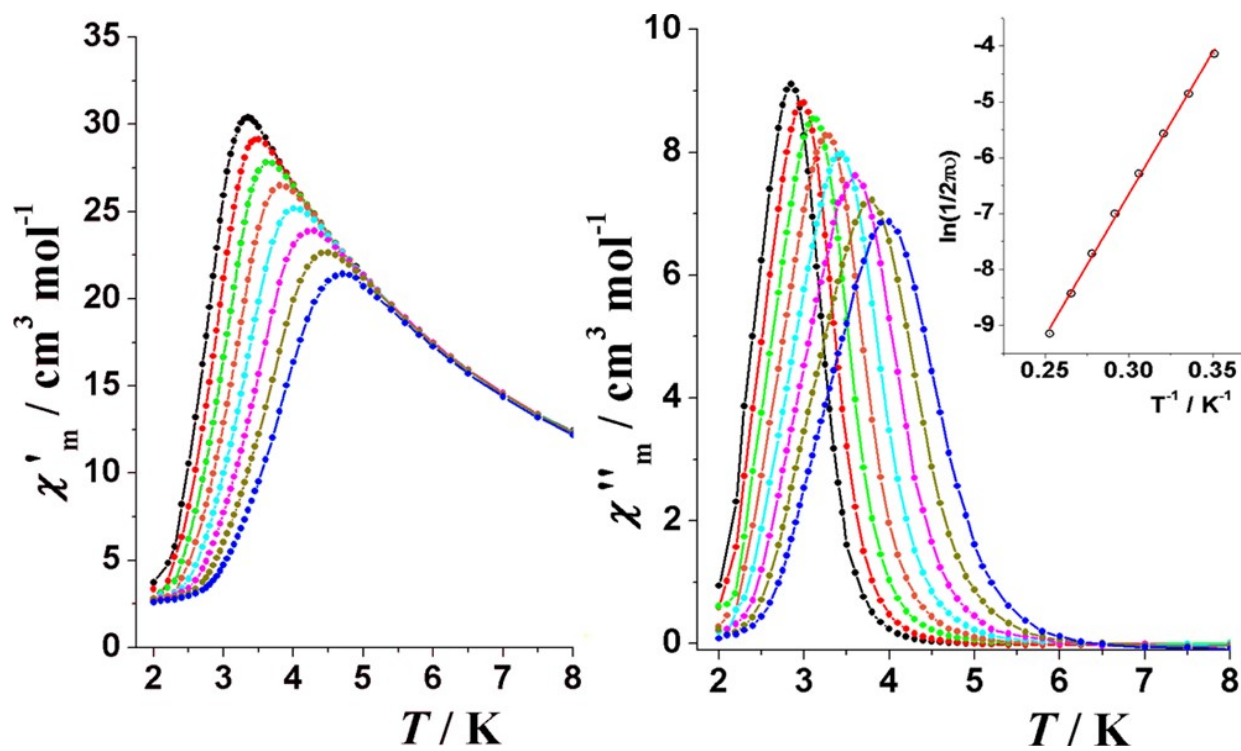


193  
194



195  
196  
197  
198

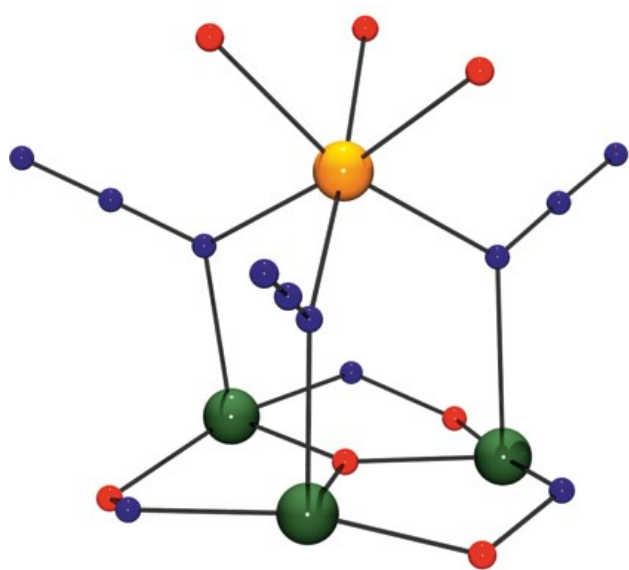
FIGURE 3



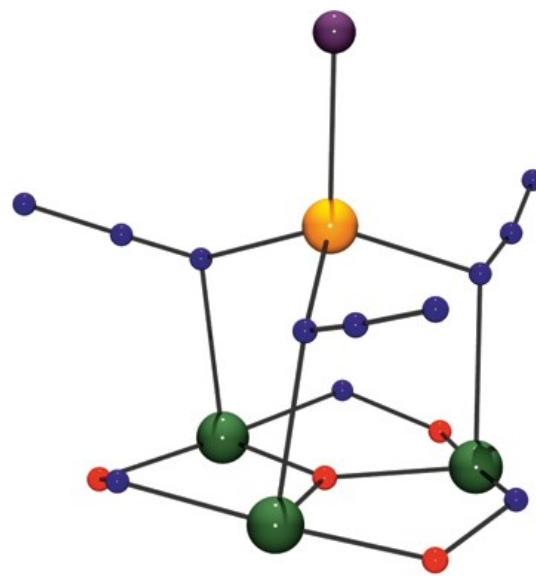
199  
200

201  
202  
203

FIGURE 4



Mn-N-Mn  $> 120^\circ$



Mn-N-Mn  $< 110^\circ$

204